



# A delayed yielding transition in mechanically annealed binary glasses at finite temperature

Nikolai V. Priezjev<sup>a,b</sup>

<sup>a</sup> Department of Mechanical and Materials Engineering, Wright State University, Dayton, OH 45435, USA

<sup>b</sup> National Research University Higher School of Economics, Moscow 101000, Russia



## ARTICLE INFO

### Keywords:

Metallic glasses  
Time periodic deformation  
Yielding transition  
Shear band  
Molecular dynamics simulations

## ABSTRACT

The influence of strain amplitude, glass stability and thermal fluctuations on shear band formation and yielding transition is studied using molecular dynamics simulations. The model binary mixture is first gradually cooled below the glass transition temperature and then periodically deformed to access a broad range of potential energy states. We find that the critical strain amplitude becomes larger for highly annealed glasses within about one thousand shear cycles. Moreover, upon continued loading at a fixed strain amplitude, the yielding transition is delayed in glasses mechanically annealed to lower energy states. It is also demonstrated that nucleation of a small cluster of atoms with large nonaffine displacements precedes a sharp energy change associated with the yielding transition. These results are important for thermal and mechanical processing of amorphous alloys with tunable mechanical and physical properties.

## 1. Introduction

Understanding how the disordered atomic structure of amorphous alloys evolves under thermal or mechanical treatments is important for predicting their physical and mechanical properties [1]. For instance, due to their enhanced strength, elastic limit and corrosion resistance, bulk metallic glasses become promising materials for medical and dental applications [2]. It is well understood by now that plastic deformation in disordered solids proceeds via collective rearrangements of small groups of atoms or shear transformations [3,4]. Depending on the degree of annealing, metallic glasses can become brittle and fail via sudden formation of narrow regions where strain is localized within the so-called shear bands. In turn, thermo-mechanical processing might lead to higher energy, rejuvenated states and, thus, improved plasticity [5]. The common techniques include high pressure torsion, elastostatic loading, shot peening, ion irradiation, and more recently discovered thermal cycling [5,6]. However, design and development of novel processing routes for amorphous alloys with optimized properties are impeded by the time required to explore the vast parameter space.

In recent years, the structural relaxation dynamics and yielding transition in amorphous materials under periodic loading conditions were extensively studied using atomistic simulations [7–32]. Remarkably, it was found that following a number of transient deformation cycles, the particle trajectories in a disordered solid at zero temperature become exactly reversible and fall into the so-called ‘limit

cycles’ [9,11]. In general, the potential energy of thermal glasses can be reduced during small-amplitude periodic loading via a series of collective, irreversible rearrangements of atoms, in a process termed ‘mechanical annealing’ [18,20–25,29]. By contrast, the oscillatory deformation at sufficiently large strain amplitudes leads to the formation of shear bands, while the onset of yielding is accelerated at higher temperatures, larger strain amplitudes, or due to alternating shear orientation [8,13,15,16,19,23,24,27,32]. More recently, it was demonstrated that the critical strain amplitude at zero temperature becomes larger in highly stable glasses obtained using either the swap Monte Carlo algorithm [30] or mechanical annealing [31]. In spite of these efforts, however, the interplay between glass stability, thermal fluctuations, and mechanical deformation in relation to strain localization and yielding remains largely unexplored.

In this paper, the effects of temperature, degree of annealing, and strain amplitude on the yielding transition in amorphous alloys are investigated using molecular dynamics simulations. The model glass is represented by the binary mixture, which is gradually cooled below the glass transition temperature and then further annealed via small-amplitude cyclic loading to progressively lower energy states. It will be shown that the critical strain amplitude increases for more stable glasses loaded during about one thousand cycles at finite temperatures. On the other hand, the yielding transition is delayed in lower energy glasses subjected to thousands of shear cycles with a fixed strain amplitude.

E-mail address: [nikolai.priezjev@wright.edu](mailto:nikolai.priezjev@wright.edu).

The contents of this paper are as follows. We describe the details of molecular dynamics simulations and the deformation protocol in the next section. The numerical results for the mechanical annealing, potential energy, mechanical properties, and shear band formation during the yielding transition in periodically driven binary glasses are presented in Section 3. The brief summary is given in the last section.

## 2. Molecular dynamics (MD) simulations

The composition of the amorphous alloy consists of (80:20) binary mixture with strongly non-additive interaction between different types of atoms, which suppresses crystallization upon cooling [33]. The model was introduced by Kob and Andersen (KA) about twenty years ago and has since been extensively studied by a number of groups [33]. In the KA model, the interaction between any two atoms is specified via the Lennard-Jones (LJ) potential:

$$V_{\alpha\beta}(r) = 4\varepsilon_{\alpha\beta} \left[ \left( \frac{\sigma_{\alpha\beta}}{r} \right)^{12} - \left( \frac{\sigma_{\alpha\beta}}{r} \right)^6 \right], \quad (1)$$

with the parameters:  $\varepsilon_{AA} = 1.0$ ,  $\varepsilon_{AB} = 1.5$ ,  $\varepsilon_{BB} = 0.5$ ,  $\sigma_{AA} = 1.0$ ,  $\sigma_{AB} = 0.8$ ,  $\sigma_{BB} = 0.88$ , and  $m_A = m_B$  [33]. We note that this parametrization is similar to the description of the amorphous metal-metalloid alloy Ni<sub>80</sub>P<sub>20</sub> studied by Weber and Stillinger [34]. In the present study, the LJ potential was truncated at the cutoff radius  $r_{c,\alpha\beta} = 2.5\sigma_{\alpha\beta}$  to reduce computational efforts. The simulation domain contains 48 000 type A atoms and 12 000 type B atoms, and the total number of atoms 60 000 is kept fixed. The following reduced units of length, mass, and energy  $\sigma = \sigma_{AA}$ ,  $m = m_A$ , and  $\varepsilon = \varepsilon_{AA}$  were used for all physical quantities. Furthermore, the velocity Verlet algorithm with the time step  $\Delta t_{MD} = 0.005\tau$  was employed for the numerical integration of the equations of motion [35,36]. Here,  $\tau = \sigma\sqrt{m}/\varepsilon$  is the characteristic LJ time.

The binary mixture was first thoroughly equilibrated at the temperature  $T_{LJ} = 1.0\varepsilon/k_B$  and density  $\rho = \rho_A + \rho_B = 1.2\sigma^{-3}$ . Here,  $k_B$  denotes the Boltzmann constant. For reference, the critical temperature of the KA model at this density is  $T_c = 0.435\varepsilon/k_B$  [33]. The temperature was regulated via the Nosé-Hoover thermostat [35,36]. All simulations were carried out at the constant volume, and the size of the periodic box was fixed to  $L = 36.84\sigma$ . Following the equilibration period, the system was linearly cooled below the glass transition at the rate  $10^{-5}\varepsilon/k_B\tau$  to  $T_{LJ} = 0.30\varepsilon/k_B$ .

In order to access lower potential energy states, periodic shear deformation along the  $xz$  plane was imposed as follows:

$$\gamma(t) = \gamma_0 \sin(2\pi t/T), \quad (2)$$

where  $\gamma_0$  is the strain amplitude and  $T = 5000\tau$  is the oscillation period. The cyclic loading was first applied at  $T_{LJ} = 0.30\varepsilon/k_B$  and the strain amplitude  $\gamma_0 = 0.035$ . It was previously shown that this value of strain amplitude is below the yielding strain at  $T_{LJ} = 0.30\varepsilon/k_B$  and  $\rho = 1.2\sigma^{-3}$ , and the relaxation rate (the potential energy decrease over time) is relatively large [21]. Further, the dynamic response of the annealed glass to oscillatory shear deformation was investigated at two temperatures, namely,  $T_{LJ} = 0.1\varepsilon/k_B$  and  $0.01\varepsilon/k_B$ . Due to computational limitations, the MD simulations were performed only for one sample. The typical production run during 3400 cycles with the period  $T = 5000\tau$  required about 94 days using 40 processors in parallel.

## 3. Results

Amorphous alloys like metallic glasses are typically formed upon rapid cooling across the glass transition temperature, and, due to the absence of topological defects, the yield stress during deformation is relatively large [37]. The stress overshoot can be further increased by relocating the glass to lower potential energy states via thermal or mechanical annealing [5]. In particular, it was recently shown that the critical strain amplitude increases in well annealed glasses subjected to

athermal quasistatic cyclic shear deformation [30,31]. While in athermal simulations particle trajectories become exactly reversible (after a certain number of cycles) at strain amplitudes below the yielding transition, the periodic deformation at finite temperatures might instead lead to a delay in yielding. In other words, the number of cycles required to form a shear band in the presence of thermal fluctuations might depend on the degree of annealing as well as the strain amplitude. In what follows, the dynamic behavior of periodically deformed binary glasses is studied at strain amplitudes in the vicinity of the yielding transition at finite temperatures and in a wide range of potential energy states.

The potential energy per atom at the end of each cycle is reported in Fig. 1 for the strain amplitude  $\gamma_0 = 0.035$  and temperature  $T_{LJ} = 0.30\varepsilon/k_B$ . Note that the black line in Fig. 1 denotes the energy minima when the imposed strain is zero. It is clearly seen that the potential energy continues to decay monotonically with increasing cycle number, and the plateau level is yet to be reached. The energy decrease during 3400 cycles at  $T_{LJ} = 0.30\varepsilon/k_B$  is  $\Delta U \approx 0.046\varepsilon$ . Next, after a certain number of cycles when strain is zero, the binary glass was cooled from  $T_{LJ} = 0.30\varepsilon/k_B$  to either  $T_{LJ} = 0.10\varepsilon/k_B$  or  $0.01\varepsilon/k_B$  during the time interval  $10^4\tau$ . The resulting energy levels at the selected cycles are shown in Fig. 1 by red circles and blue squares, respectively. As is evident, the slopes of the energy decay are nearly the same at all temperatures indicating that the inherent structure remains essentially unchanged upon cooling to lower temperatures. In the following, the yielding transition and strain localization during oscillatory shear deformation will be examined at two temperatures,  $T_{LJ} = 0.10\varepsilon/k_B$  and  $0.01\varepsilon/k_B$ , well below the glass transition temperature  $\approx 0.435\varepsilon/k_B$ .

We first evaluate the mechanical properties of steadily sheared glasses and their dependence on the degree of annealing. After the amorphous system was brought from  $T_{LJ} = 0.30\varepsilon/k_B$  to  $0.10\varepsilon/k_B$  during  $10^4\tau$ , the shear modulus,  $G$ , and the peak value of the stress overshoot,  $\sigma_Y$ , were measured during startup continuous shear deformation with the strain rate  $\dot{\gamma} = 10^{-5}\tau^{-1}$  at constant volume. The shear modulus was computed at strains  $\gamma \leq 0.01$  for each shear orientation, i.e., along the  $xz$ ,  $xy$ , and  $yz$  planes. The results are presented in Fig. 2. It can be seen that both  $G$  and  $\sigma_Y$  gradually increase as a function of the cycle number. This trend is consistent with the decrease in potential energy at  $T_{LJ} = 0.10\varepsilon/k_B$  reported in Fig. 1. In other words, the shear modulus and yield stress are greater in better annealed glasses (see Fig. 3). Note also

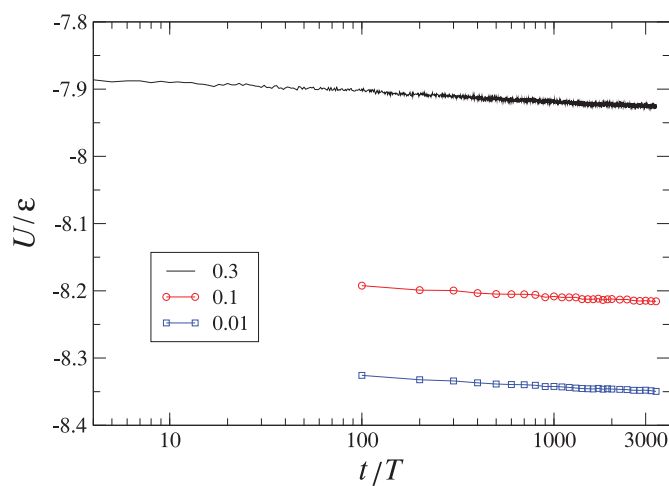


**Fig. 1.** (Color online) The potential energy minima (at zero strain) during cyclic shear with the strain amplitude  $\gamma_0 = 0.035$  at the temperature  $T_{LJ} = 0.3\varepsilon/k_B$  (black line). The potential energy of binary glasses (at zero strain) annealed to the temperatures  $T_{LJ} = 0.1\varepsilon/k_B$  (red circles) and  $T_{LJ} = 0.01\varepsilon/k_B$  (blue squares). The period of oscillation is  $T = 5000\tau$ . (For interpretation of the references to color in this figure legend, the reader is referred to the web version of this article.)

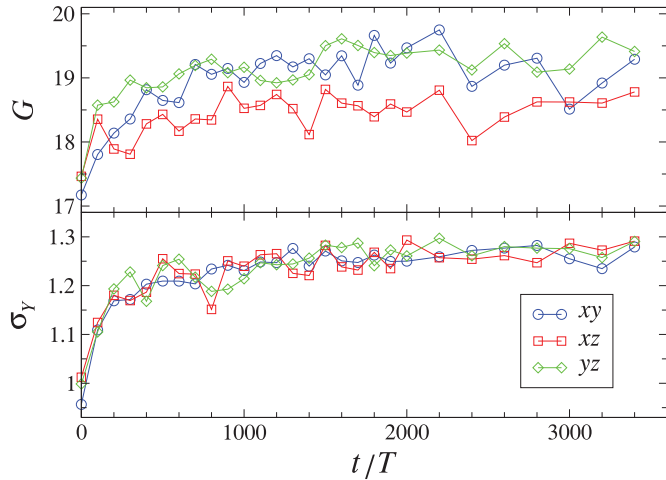


**Fig. 2.** (Color online) The shear modulus  $G$  (in units of  $\epsilon\sigma^{-3}$ ) and the yielding peak  $\sigma_Y$  (in units of  $\epsilon\sigma^{-3}$ ) versus cycle number at the temperature  $T_{LJ} = 0.1 \epsilon/k_B$ . The startup continuous shear deformation with the strain rate  $\dot{\gamma} = 10^{-5} \tau^{-1}$  is applied along the  $xy$  plane (blue circles),  $xz$  plane (red squares), and  $yz$  plane (green diamonds). (For interpretation of the references to color in this figure legend, the reader is referred to the web version of this article.)

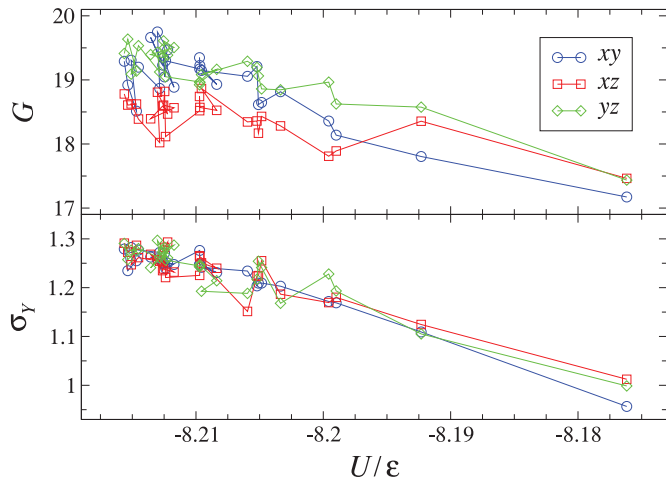


**Fig. 3.** (Color online) The dependence of the shear modulus  $G$  (in units of  $\epsilon\sigma^{-3}$ ) and the yielding peak  $\sigma_Y$  (in units of  $\epsilon\sigma^{-3}$ ) as a function of the potential energy  $U/\epsilon$  (when strain is zero) at the temperature  $T_{LJ} = 0.1 \epsilon/k_B$ . The glass is strained along the  $xy$  plane (blue circles),  $xz$  plane (red squares), and  $yz$  plane (green diamonds). The strain rate is  $\dot{\gamma} = 10^{-5} \tau^{-1}$ . The same data as in Figs. 1 and 2. (For interpretation of the references to color in this figure legend, the reader is referred to the web version of this article.)

that on average  $G_{xz}$  is smaller than  $G_{xy}$  and  $G_{yz}$ . The slight shear modulus anisotropy arises due to a finite annealing time ( $10^4 \tau$ ) after the system was periodically deformed along the  $xz$  plane at  $T_{LJ} = 0.30 \epsilon/k_B$ .

The dynamic response of the binary glass to periodic shear deformation with strain amplitudes in the range  $0.050 \leq \gamma_0 \leq 0.060$  was first probed at the temperature  $T_{LJ} = 0.10 \epsilon/k_B$ . The variation of the potential energy for thermally and mechanically annealed glasses are shown in Figs. 4 and 5, respectively. In the former case, the glass was cooled from  $T_{LJ} = 1.0 \epsilon/k_B$  to  $0.1 \epsilon/k_B$  with the rate  $10^{-5} \epsilon/k_B \tau$ , while in the latter case, the glass was first periodically strained during 300 cycles with  $\gamma_0 = 0.035$  at  $T_{LJ} = 0.3 \epsilon/k_B$  and only then brought to  $T_{LJ} = 0.1 \epsilon/k_B$  during  $10^4 \tau$ . To facilitate comparison, both vertical and horizontal scales in Figs. 4 and 5 are kept the same. It can be clearly observed that the potential energy (the plateau level before yielding) of the mechanically annealed glass is reduced (by about  $\Delta U \approx 0.025 \epsilon$ ),

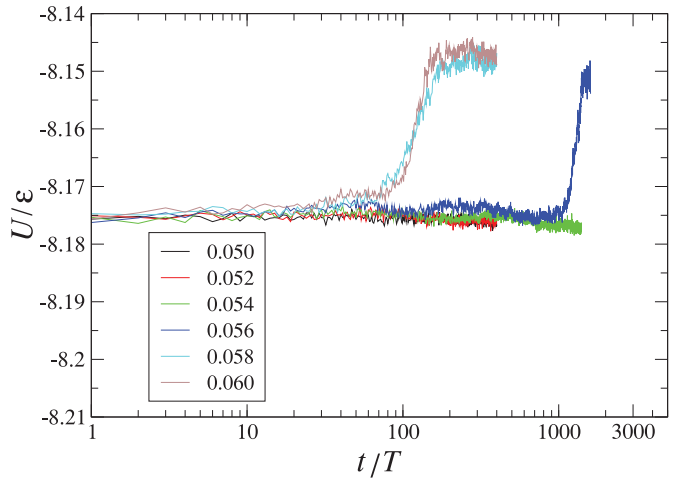


**Fig. 4.** (Color online) The time dependence of the potential energy during periodic loading at  $T_{LJ} = 0.1 \epsilon/k_B$  for the indicated values of the strain amplitude. The glass was initially prepared by cooling with the rate  $10^{-5} \epsilon/k_B \tau$  from  $T_{LJ} = 1.0 \epsilon/k_B$  to  $0.1 \epsilon/k_B$  (without mechanical annealing at  $T_{LJ} = 0.3 \epsilon/k_B$ ). The period of shear deformation is  $T = 5000 \tau$ .

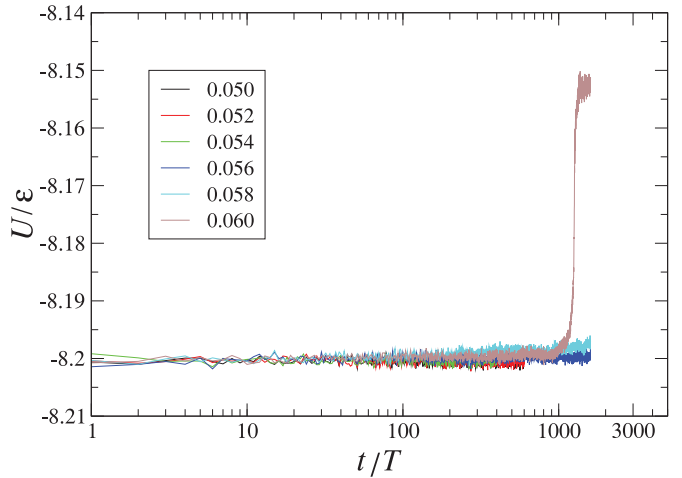


**Fig. 5.** (Color online) The variation of the potential energy minima (at zero strain) during oscillatory shear at  $T_{LJ} = 0.1 \epsilon/k_B$ . The values of the strain amplitude are listed in the inset. The glass was first loaded during 300 cycles with  $\gamma_0 = 0.035$  at  $T_{LJ} = 0.3 \epsilon/k_B$  and then brought to the temperature  $T_{LJ} = 0.1 \epsilon/k_B$  (see text for details).

and the critical strain amplitude increases. More specifically, the critical strain amplitude of the yielding transition is in the range  $0.054 < \gamma_0 < 0.056$  in Fig. 4, whereas the critical value becomes  $0.058 < \gamma_0 < 0.060$  in Fig. 5. Note that the upper bounds for the critical strain amplitude were determined from the sharp increase of the potential energy curves due to the formation of a shear band. It should be emphasized that these conclusions hold for periodic loading during 1600 cycles. In principle, the critical value of the strain amplitude might be further reduced in both cases if samples were deformed over additional cycles.

It should be mentioned that the characteristic increase in potential energy above the critical strain amplitude, which is associated with the formation of a system-spanning shear band, was repeatedly reported in the previous MD studies [15,16,19,24,27,30–32]. In particular, it was demonstrated that although the atomic density within a shear band is slightly reduced and the potential energy locally increases, the glass outside the shear band continues annealing upon subsequent periodic deformation with an effectively lower strain amplitude [24]. Generally, the formation of a shear band at finite temperatures is delayed for cyclic

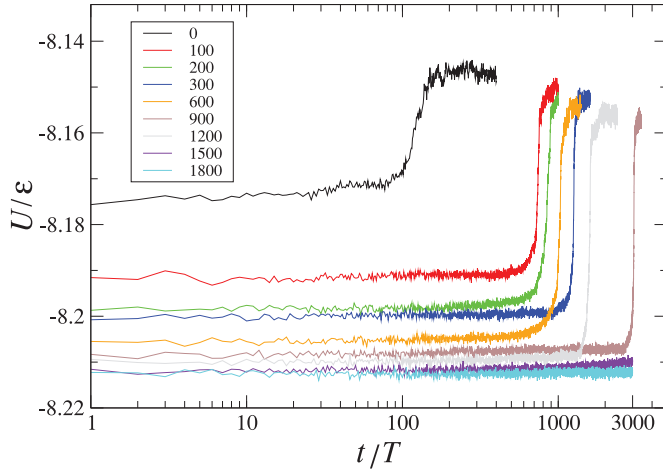


**Fig. 6.** (Color online) The potential energy versus cycle number for the strain amplitude  $\gamma_0 = 0.060$  and temperature  $T_{LJ} = 0.1 \varepsilon/k_B$ . The number of cycles used for mechanical annealing at  $T_{LJ} = 0.3 \varepsilon/k_B$  and  $\gamma_0 = 0.035$  are listed in the legend.

loading above the yielding strain amplitude for glasses prepared with slower cooling rates [27]. More recently, it was also shown that alternating shear orientation promotes the formation of shear bands in amorphous alloys subjected to periodic deformation [32].

We next report the potential energy as a function of the number of cycles at the strain amplitude  $\gamma_0 = 0.060$  and temperature  $T_{LJ} = 0.1 \varepsilon/k_B$  in Fig. 6. Here, different curves denote the potential energy at the end of each cycle for glasses that were periodically deformed at  $T_{LJ} = 0.30 \varepsilon/k_B$  for the specified number of cycles (listed in the inset). Thus, the data for zero and 300 cycles are same as in Figs. 4 and 5. The results presented in Fig. 6 demonstrate that the yielding transition is delayed for glasses that were mechanically annealed to lower energy levels. Note, however, that the number of cycles before the transition is not always larger for lower energy states. For example, the glass initially at  $U \approx -8.20 \varepsilon$  yields after about 1250 cycles (the blue curve), while for  $U \approx -8.205 \varepsilon$ , the transition occurs after about 1000 cycles (the orange curve). Furthermore, the system dynamics remains nearly reversible during 3000 cycles at the two lowest energy states, leaving the possibility of yielding under continued loading.

Similar results are also observed in Fig. 7 for cyclic loading with the strain amplitude  $\gamma_0 = 0.080$  at the lower temperature  $T_{LJ} = 0.01 \varepsilon/k_B$ . It was previously demonstrated that the strain amplitude  $\gamma_0 = 0.075$  is

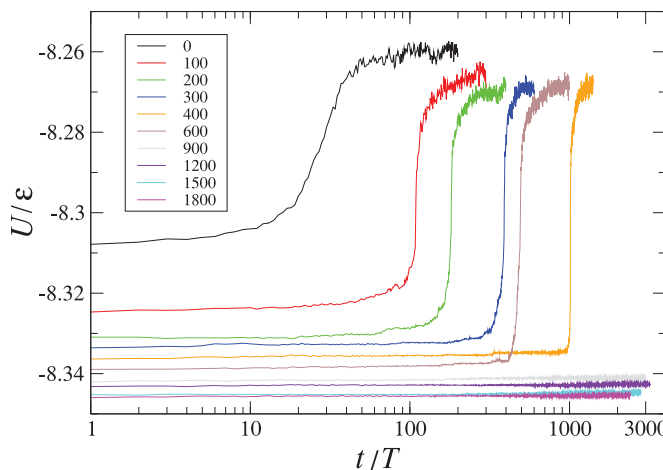


**Fig. 7.** (Color online) The dependence of the potential energy as a function of the cycle number during periodic deformation with the strain amplitude  $\gamma_0 = 0.080$  at the temperature  $T_{LJ} = 0.01 \varepsilon/k_B$ . The legend shows the number of ‘annealing’ cycles at  $T_{LJ} = 0.3 \varepsilon/k_B$  (see text for details).

above the critical amplitude for periodic shear deformation of the KA mixture at the density  $\rho = 1.2 \sigma^{-3}$  and cooling rates from  $10^{-2}$  to  $10^{-5} \varepsilon/k_B \tau$  [27]. For reference, the lowest potential energy in the KA glass cooled at  $10^{-2} \varepsilon/k_B \tau$  and then periodically deformed during thousands of shear cycles at  $T_{LJ} = 0.01 \varepsilon/k_B$  is  $U \approx -8.286 \varepsilon$  [32]. As shown in Fig. 7, the number of cycles until yielding increases roughly tenfold for lower energy glasses, whereas at  $U \lesssim -8.34 \varepsilon$  the deformation remains reversible during  $\approx 3000$  cycles. Note that due to reduced thermal fluctuations at  $T_{LJ} = 0.01 \varepsilon/k_B$ , the appearance of discrete steps in the potential energy before the yielding transition becomes more evident. As discussed below, the slight increase in the potential energy is associated with nucleation of small clusters of atoms with irreversible trajectories.

Further insights into the microscopic dynamics of atoms during cyclic deformation can be gained by inspecting the so-called nonaffine displacements. Briefly, the deviation from the affine deformation for a group of atoms can be quantified via the nonaffine measure  $D^2(t, \Delta t)$ , which is defined via the transformation matrix  $J_i$  as follows:

$$D^2(t, \Delta t) = \frac{1}{N_i} \sum_{j=1}^{N_i} \left\{ \mathbf{r}_j(t + \Delta t) - \mathbf{r}_i(t + \Delta t) - J_i \left[ \mathbf{r}_j(t) - \mathbf{r}_i(t) \right] \right\}^2, \quad (3)$$

where  $\Delta t$  is the time interval between successive positions of  $N_i$  atoms, and the sum is taken over nearest neighbors of the  $i$ th atom [38]. The spatiotemporal analysis on nonaffine displacements of atoms was recently carried out to describe irreversible dynamics in binary glasses under various loading conditions, namely, periodic [12,14,16,18,19,25,27,32] and startup continuous [39–43] shear deformation, tension-compression loading [20,29], elastostatic loading [44], as well as thermal cycling [45–48].

The sequence of snapshots of atomic configurations are presented in Fig. 8 (a-d). The data are taken during periodic deformation with the strain amplitude  $\gamma_0 = 0.060$  at  $T_{LJ} = 0.1 \varepsilon/k_B$  (denoted by the grey curve in Fig. 6). The corresponding energy levels along the grey curve are (a)  $U \approx -8.209 \varepsilon$  at  $t = 1000 T$ , (b)  $-8.203 \varepsilon$  at  $1500 T$ , (c)  $-8.179 \varepsilon$  at  $1600 T$ , and (d)  $-8.155 \varepsilon$  at  $2000 T$ . The parameter  $D^2(t, \Delta t = T)$  is computed for two consecutive configurations at zero strain. For visualization of irreversible domains, only atoms with relatively large nonaffine displacements,  $D^2(t, T) > 0.04 \sigma^2$ , are displayed in Fig. 8. Note that the typical cage size in the KA mixture at  $\rho = 1.2 \sigma^{-3}$  is about  $0.1 \sigma$ , and, therefore, empty regions in Fig. 8 correspond to spatial domains with nearly reversible dynamics.

It can be readily observed in Fig. 8 (a) that reversible deformation involves only a small number of isolated atoms (mostly B type) with large nonaffine displacements. In this case, the reversible deformation of the well-annealed glass continues for about 1300 cycles at the nearly constant energy level  $U \approx -8.209 \varepsilon$ . In turn, the slight increase in potential energy is associated with the nucleation of a cluster of atoms with irreversible displacements, as shown in Fig. 8 (b). Furthermore, at about midway between two energy levels, the formation of a shear band proceeds along the  $xy$  plane via periodic boundary conditions, as illustrated in Fig. 8 (c). Notice that the nonaffine measure varies gradually across the partially formed shear band. When the shear band is fully developed in Fig. 8 (d), the potential energy levels out at the plateau,  $U \approx -8.155 \varepsilon$ , and the steady-state deformation involves two well separated domains with diffusive and reversible dynamics.

Qualitatively similar results were observed during cyclic loading with the strain amplitude  $\gamma_0 = 0.080$  at the lower temperature  $T_{LJ} = 0.01 \varepsilon/k_B$ . The selected snapshots in Fig. 9 illustrate the process of shear band formation in the well-annealed glass described by the brown curve in Fig. 7. The potential energy values at zero strain are (a)  $U \approx -8.337 \varepsilon$  at  $t = 300 T$ , (b)  $-8.328 \varepsilon$  at  $460 T$ , (c)  $-8.310 \varepsilon$  at  $487 T$ , and (d)  $-8.268 \varepsilon$  at  $800 T$ . The first indication of the approaching transition is reflected in the slight increase of the potential energy after about 150 cycles (the brown curve in Fig. 7), which corresponds to the formation of the cluster of about 30 atoms shown in Fig. 9 (a). When  $U$

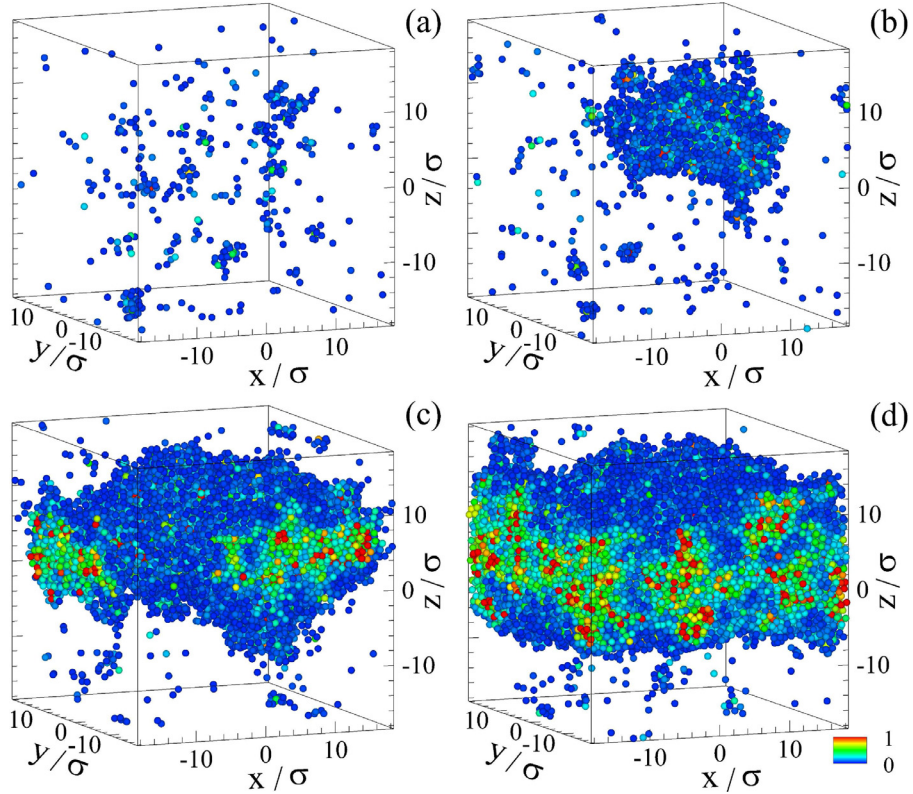


**Fig. 8.** (Color online) The selected snapshots of atomic configurations during periodic shear with the strain amplitude  $\gamma_0 = 0.060$  at the temperature  $T_{LJ} = 0.1 \varepsilon/k_B$ . The nonaffine measure is (a)  $D^2(1000 T, T) > 0.04 \sigma^2$ , (b)  $D^2(1500 T, T) > 0.04 \sigma^2$ , (c)  $D^2(1600 T, T) > 0.04 \sigma^2$ , and (d)  $D^2(2000 T, T) > 0.04 \sigma^2$ . The legend indicates the magnitude of  $D^2$ . The oscillation period is  $T = 5000 \tau$ . Atoms are not drawn to scale.

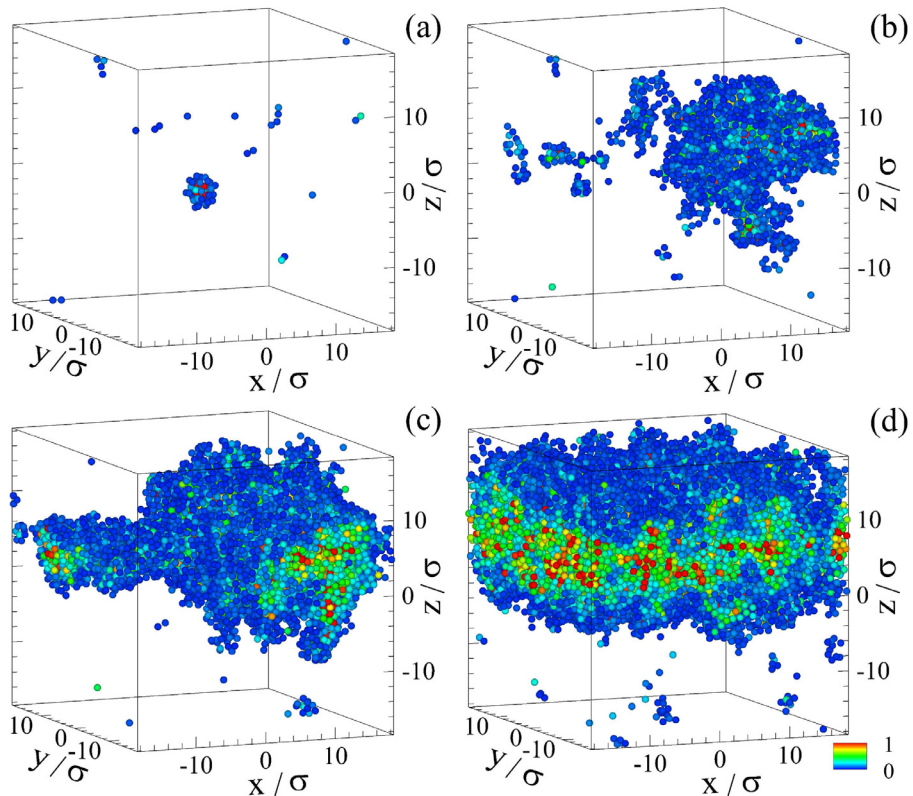


**Fig. 9.** (Color online) The positions of atoms at zero strain during periodic loading with the strain amplitude  $\gamma_0 = 0.080$  at the temperature  $T_{LJ} = 0.01 \varepsilon/k_B$ . The nonaffine quantity is (a)  $D^2(300 T, T) > 0.04 \sigma^2$ , (b)  $D^2(460 T, T) > 0.04 \sigma^2$ , (c)  $D^2(487 T, T) > 0.04 \sigma^2$ , and (d)  $D^2(800 T, T) > 0.04 \sigma^2$ . The magnitude of  $D^2$  is defined by the colorcode in the legend.

increases by about 15% of the threshold energy at the yielding transition, the cluster increases significantly but remains compact, as displayed in Fig. 9 (b). Upon further loading, a tube-like structure is formed along the  $y$  axis and then a narrow arm gets extended along the  $x$  direction [ see Fig. 9 (c) ]. Finally, after the transition, periodically driven glass contains the shear band along the  $xy$  plane with the thickness of about half the box size, as shown in Fig. 9 (d). Hence, the nucleation of small clusters of atoms with irreversible trajectories and the corresponding discrete steps in the potential energy curves demonstrate that the location of a shear band across a system can be predicted at least several cycles before the yielding transition.

#### 4. Conclusions

In summary, molecular dynamics simulations were performed to investigate the influence of glass stability, temperature, and strain amplitude on reversibility and yielding transition in cyclically loaded amorphous materials. The model glass consists of a mixture of two types of atoms with strongly non-additive interactions, which forms a disordered solid when gradually cooled below the glass transition temperature. A wide range of potential energy states were accessed via small-amplitude periodic deformation during thousands of shear cycles. It was shown that both the shear modulus and peak value of the stress overshoot increase in more stable glasses. Furthermore, we found that the critical strain amplitude increases in glasses mechanically annealed to lower potential energies when periodically deformed for about one thousand shear cycles at a finite temperature. At the same time, if the strain amplitude is fixed, the yielding transition is delayed in highly annealed glasses deformed over thousands of cycles. The spatial analysis of nonaffine displacements elucidates the process of strain localization, which includes a nucleation of a small cluster of atoms with irreversible trajectories, followed by propagation of a shear band along a plane.

#### Declaration of Competing Interest

The authors declare that they have no known competing financial interests or personal relationships that could have appeared to influence the work reported in this paper.

#### Acknowledgments

Financial support from the National Science Foundation (CNS-1531923) is gratefully acknowledged. The article was prepared within the framework of the HSE University Basic Research Program and funded in part by the Russian Academic Excellence Project ‘5-100’. The numerical simulations were carried out at Wright State University’s Computing Facility and the Ohio Supercomputer Center. The molecular dynamics simulations were carried out using the efficient LAMMPS code developed at Sandia National Laboratories [35].

#### References

- [1] J.C. Qiao, Q. Wang, J.M. Pelletier, H. Kato, R. Casalini, D. Crespo, E. Pineda, Y. Yao, Y. Yang, Structural heterogeneities and mechanical behavior of amorphous alloys, *Prog. Mater. Sci.* 104 (2019) 250.
- [2] K. Imai, X. Zhou, X. Liu, Application of Zr and Ti-based bulk metallic glasses for orthopaedic and dental device materials, *Metals* 10 (2020) 203.
- [3] F. Spaepen, A microscopic mechanism for steady state inhomogeneous flow in metallic glasses, *Acta Metall.* 25 (1977) 407.
- [4] A.S. Argon, Plastic deformation in metallic glasses, *Acta Metall.* 27 (1979) 47.
- [5] Y. Sun, A. Concustell, A.L. Greer, Thermomechanical processing of metallic glasses: extending the range of the glassy state, *Nat. Rev. Mater.* 1 (2016) 16039.
- [6] S.V. Ketov, Y.H. Sun, S. Nachum, Z. Lu, A. Checchi, A.R. Bernalin, H.Y. Bai, W.H. Wang, D.V. Louzguine-Luzgin, M.A. Carpenter, A.L. Greer, Rejuvenation of metallic glasses by non-affine thermal strain, *Nature* 524 (2015) 200.
- [7] N.V. Priezjev, Heterogeneous relaxation dynamics in amorphous materials under cyclic loading, *Phys. Rev. E* 87 (2013) 052302.
- [8] D. Fiocco, G. Foffi, S. Sastry, Oscillatory athermal quasistatic deformation of a model glass, *Phys. Rev. E* 88 (2013) 020301(R).
- [9] I. Regev, T. Lookman, C. Reichhardt, Onset of irreversibility and chaos in amorphous solids under periodic shear, *Phys. Rev. E* 88 (2013) 062401.
- [10] N.V. Priezjev, Dynamical heterogeneity in periodically deformed polymer glasses, *Phys. Rev. E* 89 (2014) 012601.
- [11] I. Regev, J. Weber, C. Reichhardt, K.A. Dahmen, T. Lookman, Reversibility and criticality in amorphous solids, *Nat. Commun.* 6 (2015) 8805.
- [12] N.V. Priezjev, Reversible plastic events during oscillatory deformation of amorphous solids, *Phys. Rev. E* 93 (2016) 013001.
- [13] T. Kawasaki, L. Berthier, Macroscopic yielding in jammed solids is accompanied by a non-equilibrium, first-order transition in particle trajectories, *Phys. Rev. E* 94 (2016) 022615.
- [14] N.V. Priezjev, Nonaffine rearrangements of atoms in deformed and quiescent binary glasses, *Phys. Rev. E* 94 (2016) 023004.
- [15] P. Leishangthem, A.D.S. Parmar, S. Sastry, The yielding transition in amorphous solids under oscillatory shear deformation, *Nat. Commun.* 8 (2017) 14653.
- [16] N.V. Priezjev, Collective nonaffine displacements in amorphous materials during large-amplitude oscillatory shear, *Phys. Rev. E* 95 (2017) 023002.
- [17] M. Fan, M. Wang, K. Zhang, Y. Liu, J. Schroers, M.D. Shattuck, C.S. O’Hern, The effects of cooling rate on particle rearrangement statistics: rapidly cooled glasses are more ductile and less reversible, *Phys. Rev. E* 95 (2017) 022611.
- [18] N.V. Priezjev, Molecular dynamics simulations of the mechanical annealing process in metallic glasses: effects of strain amplitude and temperature, *J. Non-Cryst. Solids* 479 (2018) 42.
- [19] N.V. Priezjev, The yielding transition in periodically sheared binary glasses at finite temperature, *Comput. Mater. Sci.* 150 (2018) 162.
- [20] N.V. Priezjev, Slow relaxation dynamics in binary glasses during stress-controlled, tension-compression cyclic loading, *Comput. Mater. Sci.* 153 (2018) 235.
- [21] P. Das, A.D.S. Parmar, S. Sastry, Annealing glasses by cyclic shear deformation, 2018, arXiv:1805.12476.
- [22] N.V. Priezjev, M.A. Makeev, The influence of periodic shear on structural relaxation and pore redistribution in binary glasses, *J. Non-Cryst. Solids* 506 (2019) 14.
- [23] N.V. Priezjev, M.A. Makeev, Structural transformations during periodic deformation of low-porosity amorphous materials, *Model. Simul. Mater. Sci. Eng.* 27 (2019) 025004.
- [24] A.D.S. Parmar, S. Kumar, S. Sastry, Strain localization above the yielding point in cyclically deformed glasses, *Phys. Rev. X* 9 (2019) 021018.
- [25] N.V. Priezjev, Accelerated relaxation in disordered solids under cyclic loading with alternating shear orientation, *J. Non-Cryst. Solids* 525 (2019) 119683.
- [26] E. Schinasi-Lemberg, I. Regev, Annealing and rejuvenation in a two-dimensional model amorphous solid under oscillatory shear, *Phys. Rev. E* 101 (2020) 012603.
- [27] N.V. Priezjev, Shear band formation in amorphous materials under oscillatory shear deformation, *Metals* 10 (2020) 300.
- [28] H. Li, H. Liu, H. Peng, Atomic dynamics under oscillatory shear in metallic glasses, *J. Non-Cryst. Solids* 539 (2020) 120069.
- [29] P.K. Jana, N.V. Priezjev, Structural relaxation in amorphous materials under cyclic tension-compression loading, *J. Non-Cryst. Solids* 540 (2020) 120098.
- [30] W.-T. Yeh, M. Ozawa, K. Miyazaki, T. Kawasaki, L. Berthier, Glass stability changes the nature of yielding under oscillatory shear, *Phys. Rev. Lett.* 124 (2020) 225502.
- [31] H. Bhaumik, G. Foffi, S. Sastry, The role of annealing in determining the yielding behavior of glasses under cyclic shear deformation, 2020, arXiv:1911.12957.
- [32] N.V. Priezjev, Alternating shear orientation during cyclic loading facilitates yielding in amorphous materials, 2020, arXiv:2001.06853.
- [33] W. Kob, H.C. Andersen, Testing mode-coupling theory for a supercooled binary Lennard-Jones mixture: the van hove correlation function, *Phys. Rev. E* 51 (1995) 4626.
- [34] T.A. Weber, F.H. Stillinger, Local order and structural transitions in amorphous metal-metalloid alloys, *Phys. Rev. B* 31 (1985) 1954.
- [35] S.J. Plimpton, Fast parallel algorithms for short-range molecular dynamics, *J. Comp. Phys.* 117 (1995) 1.
- [36] M.P. Allen, D.J. Tildesley, *Computer Simulation of Liquids*, Clarendon, Oxford, 1987.
- [37] Y.Q. Cheng, E. Ma, Atomic-level structure and structure-property relationship in metallic glasses, *Prog. Mater. Sci.* 56 (2011) 379.
- [38] M.L. Falk, J.S. Langer, Dynamics of viscoplastic deformation in amorphous solids, *Phys. Rev. E* 57 (1998) 7192.
- [39] G.P. Shrivastav, P. Chaudhuri, J. Horbach, Yielding of glass under shear: a directed percolation transition precedes shear-band formation, *Phys. Rev. E* 94 (2016) 042605.
- [40] R. Jana, L. Pastewka, Correlations of non-affine displacements in metallic glasses through the yield transition, *J. Phys. 2* (2019) 045006.
- [41] N.V. Priezjev, The effect of thermal history on the atomic structure and mechanical properties of amorphous alloys, *Comput. Mater. Sci.* 174 (2020) 109477.
- [42] N.V. Priezjev, Spatiotemporal analysis of nonaffine displacements in disordered solids sheared across the yielding point, *Metall. Mater. Trans. A* 51 (2020) 3713.
- [43] M. Singh, M. Ozawa, L. Berthier, Brittle yielding of amorphous solids at finite shear rates, *Phys. Rev. Mater.* 4 (2020) 025603.
- [44] N.V. Priezjev, Aging and rejuvenation during elastostatic loading of amorphous alloys: a molecular dynamics simulation study, *Comput. Mater. Sci.* 168 (2019) 125.
- [45] N.V. Priezjev, Atomistic modeling of heat treatment processes for tuning the mechanical properties of disordered solids, *J. Non-Cryst. Solids* 518 (2019) 128.
- [46] N.V. Priezjev, The effect of cryogenic thermal cycling on aging, rejuvenation, and mechanical properties of metallic glasses, *J. Non-Cryst. Solids* 503 (2019) 131.
- [47] Q.-L. Liu, N.V. Priezjev, The influence of complex thermal treatment on mechanical properties of amorphous materials, *Comput. Mater. Sci.* 161 (2019) 93.
- [48] N.V. Priezjev, Potential energy states and mechanical properties of thermally cycled binary glasses, *J. Mater. Res.* 34 (2019) 2664.